

Photoluminescence Enhancement and Morphological Properties of Carbon Codoped GaN:Er

M.E Overberg¹, C.R. Abernathy¹, S. J. Pearton¹, R. G. Wilson², and J. M. Zavada³

¹Department of Materials Science and Engineering, University of Florida
Gainesville, FL 32611, U. S. A.

²Consultant
Stevenson Ranch, CA 91381, U. S. A.

³U. S. Army European Research Office
London, NW1 5 TH, U. K.

ABSTRACT

The surface morphology and the room temperature 1.54 μm photoluminescence (PL) intensity from GaN:Er grown by gas source molecular beam epitaxy have been investigated as a function of C concentration as introduced by CBr_4 . Similar to previous results with increasing Er level, increasing the C concentration initially improved the surface smoothness as measured by atomic force microscopy (AFM) and scanning electron microscopy (SEM), with RMS roughness improving by a factor of seven over undoped GaN. The PL also improved dramatically. However, the highest amounts of C investigated produced a decrease in the PL as well as a roughening of the film surface. These effects indicate that the GaN:Er had reached its C solubility limit, producing an increased amount of defect induced nonradiative recombination.

INTRODUCTION

Recently, there has been an increasing amount of research in rare earth doped semiconductors for optoelectronics. As opposed to traditional light emitters that rely on conduction band edge recombination to produce photons, rare earth doped (RE) materials utilize electronic transitions involving the 4f shells of the rare earth element. With REs, the emission wavelength is most insensitive as the 4f shells are well shielded from the atomic bonding 5s and 5p shells. RE doping has been investigated in several semiconductor systems with various degrees of success [1-4]. While the emission wavelength is most material insensitive, the emission intensity is not. In particular, the larger the bandgap and the more ionic the semiconductor, the greater the RE luminescence [5,6]. The wide bandgap III-nitrides are therefore attractive as a host material, and offer the advantages of a high degree of structural and thermal stability. Already, several reports have been made of RE doping of GaN for both visible (Eu, Er, Tm) and IR emission (Pr, Er) [7-13]. Doping with Er is particularly attractive due to its 1.54 μm emission, which exploits the attenuation loss minima of silica fibers. It has been found that codopant impurities (O, C, F) can enhance the luminescence and efficiency of Si:Er [14-18], but only when introduced in the proper Er/Impurity ratio. While it has been shown that addition of elements such as C and O can enhance the IR emission from GaN:Er [8], there has as yet been no systematic investigation of the role of the concentration of these codopants in the luminescence and surface properties of the GaN films. In this work, the effect of C codoping introduced via CBr_4 on the structural and optical properties of

GaN:Er films grown on sapphire by gas source molecular beam epitaxy (GSMBE) has been investigated in an attempt to address these issues.

EXPERIMENTAL DETAILS

Films were grown by GSMBE in a modified Varian INTEVAC Gas Source Gen II on In-mounted (0001) Al₂O₃. A high temperature surface nitridation preceded all layer growth, and was performed at a temperature of 865 °C. A 10 nm low temperature AlN buffer layer ($T_g = 435$ °C) was then grown using dimethylethylamine alane (DMEAA) as the aluminum source. This was followed by a 1.2 μm GaN, GaN:Er, or GaN:Er:C layer, grown at a temperature of 750 °C. Solid source effusion cells provided the gallium (7N) and erbium (4N) fluxes, while the carbon was provided by the surface decomposition of CBr₄. The CBr₄ was injected into the growth chamber using an ultrapure helium (6N) carrier gas and a CBr₄ bubbler temperature of 0.0 °C. Reactive nitrogen for the nitridation and for the growth of both the AlN and GaN layers was provided by an SVT RF plasma source operating at 375 W of forward power and 3 sccm of N₂. The shuttered erbium cell was maintained at a temperature of 1250 °C, which corresponds to a dopant level of approximately 6×10^{21} cm⁻³ from SIMS analysis of previous results. The room temperature Er⁺³ photoluminescence at 1.54 μm (PL) was excited using the 514.5 nm line of an Ar ion laser and measured with an LN₂ cooled InGaAs photodetector. The surface morphology was characterized by atomic force microscopy (AFM) using a Digital Instruments Nanoscope III and by scanning electron microscopy (SEM) using a JEOL 6400.

DISCUSSION

The surface morphologies of the GaN:Er samples codoped with different C levels from the CBr₄ source are shown in Figure 1. SEM micrograph A shows the

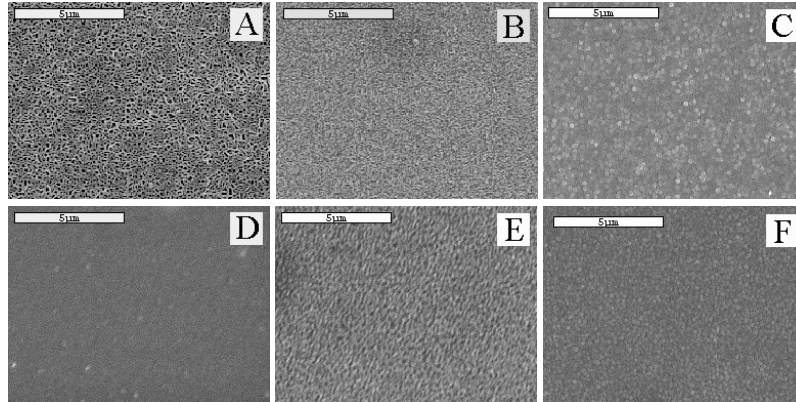


Figure 1: SEMs of GaN and GaN:Er with a progression of CBr₄ doping (CBr₄ in sccm): (A) GaN, (B) GaN:Er, (C) GaN:Er (CBr₄= 3.2×10^{-3}), (D) GaN:Er (CBr₄= 1.6×10^{-2}), (E) GaN:Er (CBr₄= 7.9×10^{-2}), and (F) GaN:Er (CBr₄= 1.6×10^{-1}).

undoped GaN surface. In micrographs B through D, as the CBr_4 flow, and therefore the C concentration, is increased, the round surface features decrease in size. A smooth morphology was obtained in GaN:Er that was codoped with roughly $1.3 \times 10^{20} \text{ cm}^{-3}$ of C. Upon further codoping, shown in micrograph E, it would appear that the round surface features then increase in size. At the highest codopant level, shown in micrograph F, they appear to decrease in size again. The C concentration in micrograph F was approximately $1.3 \times 10^{21} \text{ cm}^{-3}$. From the SEM data, it would appear that the initial increase in film smoothness is due to a reduction in the GaN domain size. GaN grown by MBE often exhibits a columnar structure that is induced by the large lattice mismatch between the GaN and the sapphire.

As with the SEM, AFM measurements of the GaN:Er surface roughness indicate an initial improvement in morphology with increasing C level, as shown in Figure 2. The RMS surface roughness of the undoped GaN film was found to be approximately 73.5 Å. Upon the addition of Er, and with subsequent C addition, the surface roughness initially decreased by a factor of seven. However, with further C addition, the surface roughness increased dramatically. It is possible that at this C concentration ($\sim 6 \times 10^{20} \text{ cm}^{-3}$), the GaN has reached its solubility limit. The increase in surface roughness could then be due to the incorporation of C in the form of defects, clusters, or precipitates. High levels of crystal defects were observed in Si:Er when the material system was “overdoped” with O [17]. With further C addition, the surface roughness drops for a CBr_4 flow of roughly 0.16 sccm. As shown in the AFM in Figure 3, rough regions and very smooth regions characterize this sample. The solid line in Figure 2 represents the overall surface roughness of the whole sample, while the dotted line represents the surface roughness of the smooth regions only. Note that there is roughly an order of magnitude drop between the two values. This suggests that coarsening effects due to increased C incorporation is opposed by surface etching of the GaN by Br left over from the CBr_4 decomposition.

When the AFM surface scans, given in Figure 3, are examined in detail, it appears that the growth mode is altered for samples A through D. These results suggest that first the Er, then the C, may interfere with the surface migration of the reactant species, resulting in a smoother, less textured surface. The obvious roughening in micrograph E gives further credence to the theory that the GaN has reached its solubility

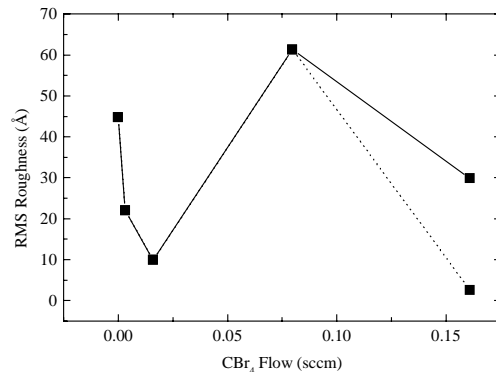


Figure 2: GaN:Er RMS roughness vs. CBr_4 flux.

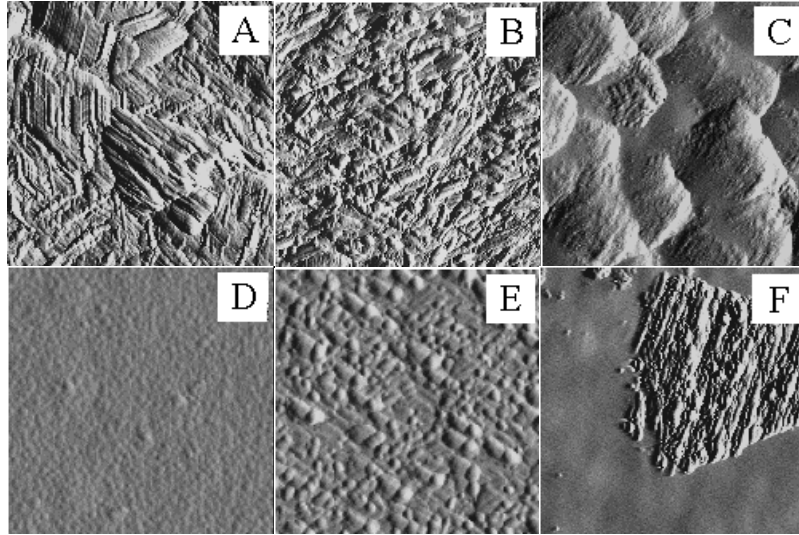


Figure 3: AFM surface scans of GaN with a progression of Er and C doping (CBr_4 flux in sccm): (A) GaN, (B) GaN:Er, (C) GaN:Er ($CBr_4=3.15 \times 10^{-3}$), (D) GaN:Er ($CBr_4=1.6 \times 10^{-2}$), (E) GaN:Er ($CBr_4=7.97 \times 10^{-2}$), and (F) GaN:Er ($CBr_4=1.6 \times 10^{-1}$). Scan dimensions were $1 \mu\text{m} \times 1 \mu\text{m} \times 5 \text{nm}$.

limit for C, and that the roughening is due to an enhanced number of defects. Finally, in micrograph F, the defect related roughening is partially compensated by Br assisted surface etching.

Figure 4 shows that the growth rate of the GaN:Er at first increases slightly with C incorporation, but then decreases as more C is added. The decrease in the growth rate at higher CBr_4 fluxes is almost certainly due to the Br species left over from the thermal decomposition of the CBr_4 at the growth surface which parasitically etches the GaN. Enhanced Br levels (and etch rates) due to the higher C fluxes will produce lower overall growth rates for the same initial GaN growth rate. Similar behavior has been observed in GaAs, GaP and AlGaAs [21].

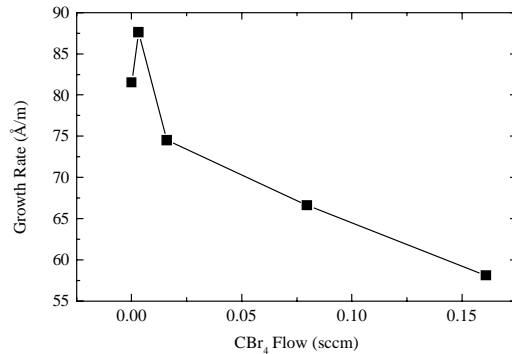


Figure 4: GaN:Er growth rate vs. CBr_4 flux.

The PL analysis, depicted in Figure 5, shows that the normalized PL intensity at first increases sharply with increased C content (over the non C-doped sample), and then decreases. This result indicates that for the Er concentration used ($\sim 6 \times 10^{21} \text{ cm}^{-3}$), the optimum codoping concentration of C is approximately $1.3 \times 10^{20} \text{ cm}^{-3}$. The initial increase in PL can be attributed to C affecting the local environment of the Er atoms. Normally, electric dipole radiation from $4f \text{ Er}^{+3}$ transitions would be forbidden due to the parity selection rule. It has been found that a noncentrosymmetric crystal field leads to parity intermixing, resulting in a finite lifetime for radiative decay. Such a crystal field can be produced by the formation of Er-C complexes, allowing efficient Er^{+3} pumping. It has also been suggested that a reduction in deep levels in the GaN, as well as enhanced promotion of Er from the +2 state to the +3 state by Er-C centers will produce a luminescence enhancement [15,17]. The decrease in the PL luminescence at high CBr_4 flows can be attributed to the further increased number of C atoms surrounding the Er producing nonradiative decay centers in the GaN matrix material. The nonradiative sites could be produced as a result of C-C clustering, precipitates, C related defects, and C atoms not linked to Er atoms. Similar results (optimum codopant level, enhanced nonradiative decay) have been seen previously in work done with Si:Er codoped with O [14,16].

CONCLUSIONS

It has been shown that GaN:Er codoped with increasing levels of C initially exhibits similar changes in surface roughness as does GaN:Er doped with increasing Er levels. Morphology initially improves, but then roughens when the GaN:Er appears to reach its C solubility limit. Growth rate and RMS roughness measurements also show that parasitic etching from Br released by CBr_4 decomposition becomes important at high CBr_4 flow rates. Finally, the integrated $1.54 \mu\text{m}$ PL intensity reaches a maximum for an optimum C concentration, similar to work done with Si:Er:O. This indicates Er-C complex formation initially increases the PL, but further codoping creates defects that enhance nonradiative recombination.

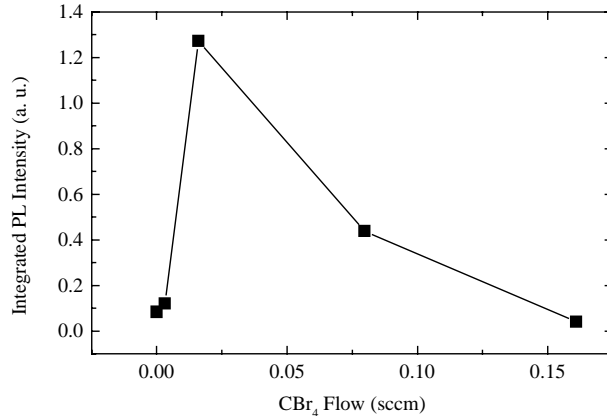


Figure 5: Integrated PL intensity of the Er^{+3} emission at $1.54 \mu\text{m}$ vs. CBr_4 flow.

ACKNOWLEDGEMENTS

The authors acknowledge the support of the U. S. Army Research Office under Contract No. DAAG55-98-1-0216. The assistance of S. M. Donovan with SEM is also greatly appreciated.

REFERENCES

1. X. Z. Wang and B. W. Wessels, *Appl. Phys. Lett.* **67**, 518 (1995).
2. H. Nakagome, K. Takahei, and Y. Homma, *J. Crystal Growth* **85**, 345 (1987).
3. J. Nakata, M. Taniguchi, and K. Takahei, *Appl. Phys. Lett.* **61**, 2665 (1992).
4. J. L. Benton, J. Michel, L. C. Kimerling, D. C. Jacobson, Y.-H. Xie, D. J. Eaglesham, E. A. Fitzgerald, and J. M. Poate, *J. Appl. Phys.* **70**, 2667 (1991).
5. P. N. Favenec, H. L'Haridon, D. Moutonnet, and Y. L. Guillo, *Electron. Lett.* **25**, 718 (1989).
6. J. M. Zavada and D. Zhang, *Solid State Electron.* **38**, 1285 (1995).
7. J. MacKenzie, C.R. Abernathy, S.J. Pearton, U. Hommerich, F. Ren, R.G. Wilson and J.M. Zavada, *Fall Materials Research Society Meeting Proceedings Vol. 468*, 123-129 (1997).
8. J. MacKenzie, C.R. Abernathy, S.J. Pearton, U. Hommerich, K. Wu, R.N. Schwartz, R.G. Wilson and J.M. Zavada, *J. Crystal Growth* **175/176**, 84-88 (1997).
9. J. D. MacKenzie, C. R. Abernathy, and S. J. Pearton, *Appl. Phys. Lett.* **72**, 2710 (1998).
10. J. Heikenfeld, M. Garter, D. S. Lee, R. Birkhahn, and A. J. Steckl, *Appl. Phys. Lett.* **75**, 1189 (1999).
11. A. J. Steckl, M. Garter, D. S. Lee, J. Heikenfeld, and R. Birkhahn, *Appl. Phys. Lett.* **75**, 2184 (1999).
12. R. Birkhahn and A. J. Steckl, *Appl. Phys. Lett.* **73**, 2143 (1998).
13. R. Birkhahn, M. Garter, and A. J. Steckl, *Appl. Phys. Lett.* **74**, 2161 (1999).
14. M. Markmann, E. Neufeld, A. Sticht, K. Brunner, G. Abstreiter, and Ch. Buchal, *Appl. Phys. Lett.* **75**, 2584 (1999).
15. S. Coffa, F. Priolo, G. Franzó, A. Polman, S. Libertino, M. Saggio, and A. Carnera, *Nucl. Instr. and Meth. in Phys. Res. B* **106**, 386 (1995).
16. F. Priolo, G. Franzó, S. Coffa, A. Polman, S. Libertino, R. Barklie, and D. Carey, *J. Appl. Phys.* **78**, 3874 (1995).
17. F. Priolo, S. Coffa, G. Franzó, C. Spinella, A. Carnera, and V. Bellani, *J. Appl. Phys.* **74**, 4936 (1993).
18. G. Franzó, S. Coffa, F. Priolo, C. Spinella, *J. Appl. Phys.* **81**, 2784 (1997).
19. J. D. MacKenzie, C. R. Abernathy, S. J. Pearton, U. Hömmerich, X. Wu, R. Schwartz, R. G. Wilson, J. M. Zavada, *J. Crystal Growth* **175/176**, 84 (1997).
20. M. E. Overberg, J. Brand, J. D. MacKenzie, C. R. Abernathy, S. J. Pearton, and J. M. Zavada, *Proc. of the State-of-the-Art Program on Comp. Semi. XXX*, *Electrochem. Soc. Proc.* **99-4**, 195-200 (1999).
21. C. R. Abernathy, J. D. MacKenzie, S. J. Pearton, and W. S. Hobson, *Appl. Phys. Lett.* **66**, 1969 (1995).